

The following resources related to this article are available online at www.sciencemag.org (this information is current as of January 1, 2010):

Updated information and services, including high-resolution figures, can be found in the online version of this article at:

<http://www.sciencemag.org/cgi/content/full/318/5850/619>

Supporting Online Material can be found at:

<http://www.sciencemag.org/cgi/content/full/318/5850/619/DC1>

This article **cites 27 articles**, 4 of which can be accessed for free:

<http://www.sciencemag.org/cgi/content/full/318/5850/619#otherarticles>

This article has been **cited by** 29 article(s) on the ISI Web of Science.

This article appears in the following **subject collections**:

Chemistry

<http://www.sciencemag.org/cgi/collection/chemistry>

Information about obtaining **reprints** of this article or about obtaining **permission to reproduce this article** in whole or in part can be found at:

<http://www.sciencemag.org/about/permissions.dtl>

was measured with a physical property measurement system. The electrical resistivity shows the MIT at $T_c = 154$ K on cooling (Fig. 1) and exhibits large thermal hysteresis behavior indicating a first-order character of the MIT. $\text{Ca}_{1.9}\text{Sr}_{0.1}\text{RuO}_4$ crystals for scanning tunneling microscopy (STM), LEED, and HREELS measurements were mounted on the sample plates with conducting silver epoxy, and a small metal post was glued on top. The crystal was cleaved by knocking off the post in ultrahigh vacuum with a base pressure of 1.0×10^{-10} torr, producing a flat shiny [001] surface that yielded a sharp LEED pattern. The STM images of the freshly cleaved surfaces show large micrometer-sized terraces. Both the LEED pattern and atomically resolved STM images indicate that the surface has a well-ordered lattice structure. All surface steps are integral multiples of ~ 6.4 Å, which is the spacing between two nearest-neighbor RuO_6 octahedron layers (Fig. 1). LEED I - V analysis shows that the surface is composed of Ca/Sr-O terminations.

13. Ismail *et al.*, *Phys. Rev. B* **67**, 035407 (2003).
14. J. H. Jung *et al.*, *Phys. Rev. Lett.* **91**, 056403 (2003).
15. A. V. Puchkov *et al.*, *Phys. Rev. Lett.* **81**, 2747 (1998).

16. S. Nakatsuji *et al.*, *Phys. Rev. Lett.* **93**, 146401 (2003).
17. Detailed spectral data analysis methods were as follows: The Drude weight is the integrated intensity obtained from the difference between the left and right sides of the quasi-elastic peak through a Lorentzian function. The phonon energy, intensity, and linewidth were obtained by fitting the phonon spectra with a Lorentzian function and were deconvoluted from the Drude tail and instrumentation-resolution function. More details of the surface phonons can be found in (32).
18. M. A. Van Hove *et al.*, *Low-Energy Electron Diffraction Experiment, Theory and Surface Structure Determination* (Springer-Verlag, Berlin, 1986).
19. V. B. Nascimento *et al.*, *Phys. Rev. B* **75**, 035408 (2007).
20. J. B. Pendry, *J. Phys. C* **13**, 937 (1980).
21. E. Heifets *et al.*, *Phys. Rev. B* **64**, 235417 (2001).
22. S. Piskunov *et al.*, *Surf. Sci.* **575**, 75 (2005).
23. Z. Fang, K. Terakura, *Phys. Rev. B* **64**, 020509 (2001).
24. Z. Fang, N. Nagaosa, K. Terakura, *Phys. Rev. B* **69**, 045116 (2004).
25. M. Pattoff, W. Nolting, *Phys. Rev. B* **59**, 2549 (1999).
26. M. Pattoff, *Adv. Solid State Phys.* **42**, 121 (2002).
27. A. Liebsch, *Phys. Rev. Lett.* **90**, 096401 (2003).

28. A. Liebsch, H. Ishida, *Phys. Rev. Lett.* **98**, 216403 (2007).
29. G. Kotliar *et al.*, *Phys. Rev. Lett.* **84**, 5180 (2000).
30. G. Kotliar, D. Vollhardt, *Phys. Today* **57**, 53 (2004).
31. S. Onoda, arXiv: cond-mat/0408297.
32. R. Moore *et al.*, *Phys. Stat. Sol. (b)* **241**, 2363 (2004).
33. Supported by the U.S. Department of Energy (DOE), Division of Materials Science and Engineering, through Oak Ridge National Laboratory. R.G.M. acknowledges support from NSF and DOE (grants NSF-DMR-0451163 and DMS&E). J.Z. thanks NSF for support under contract DMR-0346826. G.T.W. and Z.F. acknowledge support from NSF and the National Basic Research (973) Program of China. We thank A. Liebsch for many informative discussions.

Supporting Online Material

www.sciencemag.org/cgi/content/full/318/5850/615/DC1
Materials and Methods
Figs. S1 to S4
References

18 May 2007; accepted 19 September 2007
10.1126/science.1145374

A Synthetic Lectin Analog for Biomimetic Disaccharide Recognition

Yann Ferrand, Matthew P. Crump, Anthony P. Davis*

Carbohydrate recognition is biologically important but intrinsically challenging, for both nature and host-guest chemists. Saccharides are complex, subtly variable, and camouflaged by hydroxyl groups that hinder discrimination between substrate and water. We have developed a rational strategy for the biomimetic recognition of carbohydrates with all-equatorial stereochemistry (β -glucose, analogs, and homologs) and have now applied it to disaccharides such as cellobiose. Our synthetic receptor showed good affinities, not unlike those of some lectins (carbohydrate-binding proteins). Binding was demonstrated by nuclear magnetic resonance, induced circular dichroism, fluorescence spectroscopy, and calorimetry, all methods giving self-consistent results. Selectivity for the target substrates was exceptional; minor changes to disaccharide structure (for instance, cellobiose to lactose) caused almost complete suppression of complex formation.

Carbohydrates are challenging substrates for host-guest chemistry (1–4). They possess extended, complex structures that require large receptor frameworks for full encapsulation. The differences between them are often subtle (e.g., the stereochemistry of a single hydroxyl group), so that meaningful selectivity is hard to achieve. Most particularly they are found in water and, with their arrays of hydroxyl groups, they quite strongly resemble water. The first task of a receptor is to discriminate between solvent and substrate, and in the case of carbohydrates this is clearly nontrivial. There is evidence that even nature finds the problem difficult. Though critical for many biological processes (5–7), protein/carbohydrate binding is remarkably weak (8). For example, lectins, the most common class of natural receptors, quite often show affinities [association constants (K_a)] of less than 10^4 M^{-1} (9). Previous work on synthetic receptors points in the same direction.

Biomimetic (10, 11) carbohydrate receptors have been sought to model natural recognition and also for applications such as glucose sensing. However, whereas good systems are available for organic solvents (1–3, 12–15), there has been very limited success in water (1–4, 16, 17).

We have targeted carbohydrates with all-equatorial arrays of polar substituents, such as β -glucose **1** (Fig. 1). These substrates have axially directed CH groups, forming small apolar patches at top and bottom. Accordingly, our hosts incorporate roof and floor motifs composed of aromatic hydrocarbons, capable of hydrophobic attraction reinforced by CH– π interactions. These aromatic regions are supported by pillars containing polar groups that can hydrogen bond to the substrate –OH groups (Fig. 1). In prototypes of formula **2**, the roof and floor are provided by biphenyl units, and the pillars are isophthalamides. Recently, we prepared a water-soluble (18–20) variant of **2** and tested its ability to bind carbohydrates in aqueous solution (21). The system was successful but not spectacular. Glucose was bound measurably but weakly ($K_a = 9 \text{ M}^{-1}$) and with moderate selectivity (e.g., glucose:galactose = $\sim 5:1$).

Though encouraging, these properties are hardly comparable to those of lectins.

In biology, most carbohydrate recognition involves oligosaccharides, so we were interested to learn if these extended substrates could be addressed by our strategy (22–26). We therefore considered larger versions of our receptor, aimed at all-equatorial disaccharides such as cellobiose **4** (Fig. 1). We now report the design, synthesis, and study of tetracyclic disaccharide receptor **3**. This host achieves a dramatic leap in performance, showing good affinities and outstanding selectivities for its chosen substrate. It comes remarkably close to true biomimicry and provides a realistic synthetic model for protein/carbohydrate recognition.

Receptor **3** is constructed from two building blocks. A *meta*-terphenyl structure provides the roof and floor, defining the length of the cavity, and isophthalamide units serve as pillars. Each pillar includes two amide linkages, with the potential to hydrogen bond to the –OH groups in **4**. The pillars are also furnished with externally directed tricarboxylate units, to promote solubility and resist aggregation in water. An important consideration was the possibility of cavity collapse, allowing the aromatic surfaces to meet. In aqueous solution, such a process should be strongly favored, driven by hydrophobic interactions. To counter this tendency, the design incorporated five of the rigid isophthalamides, spaced fairly evenly around the terphenyl units. Molecular modeling (27, 28) confirmed that collapsed structures were strongly disfavored; all conformations found within 20 kJ mol^{-1} of the baseline possessed substantial cavities.

The receptor was synthesized from benzenoid precursors via Suzuki-Miyaura couplings and macrolactamizations (29). As expected, it dissolved freely in water to give well-resolved ^1H nuclear magnetic resonance (NMR) spectra, implying a monomeric species (fig. S4). Initial complexation studies were performed using ^1H NMR titrations with cellobiose **4** as a substrate.

School of Chemistry, University of Bristol, Cantock's Close, Bristol BS8 1TS, UK.

*To whom correspondence should be addressed. E-mail: anthony.davis@bristol.ac.uk

The spectra show clear indications of binding (Fig. 2A). Sequential disaccharide additions caused decay of the receptor spectrum and

growth of a new set of signals. These changes are consistent with complex formation, in which exchange between bound and unbound forms is

slow on the NMR time scale. As the titration proceeds, signals due to the receptor are replaced by those of the complex. The spectrum of **3** is relatively simple, reflecting its symmetry; although there are 33 aromatic protons, there are only 11 distinct environments. However, once the disaccharide is bound, all of these environments become different. Accordingly, the spectrum of the complex contains many more peaks.

The affinity of **3** for cellobiose was estimated by integration of an NMR signal from the complex against that of an internal standard (29). Errors were significant because of signal overlap, but an approximate value of $\sim 600 \text{ M}^{-1}$ could be obtained (figs. S5 and S6). To improve accuracy, binding was also investigated by induced circular dichroism (ICD) and fluorescence spectroscopy (29). The addition of cellobiose to **3** in water gave a clear ICD signal (Fig. 2B) and also a 370% increase in fluorescence output (Fig. 2C). Titration data from both methods gave excellent fits to a 1:1 binding model, with K_a values of 570 M^{-1} and 560 M^{-1} , respectively (Fig. 2D and fig. S14). For final confirmation, isothermal titration calorimetry was also applied. The fit to a 1:1 model was again good, with $K_a = 650 \text{ M}^{-1}$, change in enthalpy $\Delta H = -3.22 \text{ kcal mol}^{-1}$, and $T\Delta S = 0.62 \text{ kcal mol}^{-1}$ (where T is temperature and ΔS is the change in entropy) (fig. S15). Complex formation is mainly enthalpically driven and therefore not dominated by the classical (entropy-driven) hydrophobic effect (30). The balance between enthalpy and entropy lies comfortably within the range observed for lectins (9), supporting a lectin-like binding mode involving both hydrogen bonding and apolar interactions (31).

NMR studies yielded quite detailed structural information about the complex. Two-dimensional

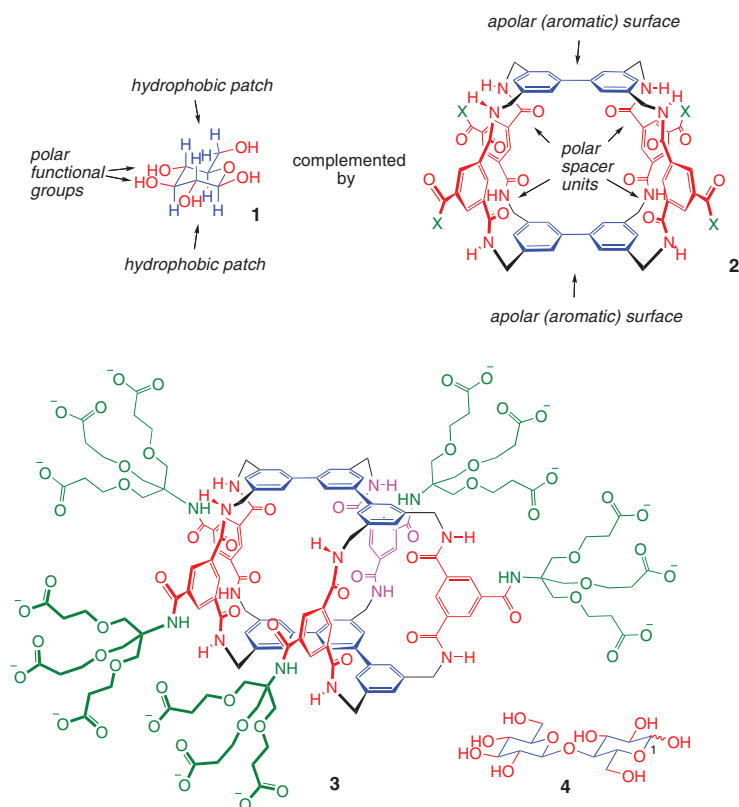


Fig. 1. The design of receptors for all-equatorial carbohydrates. **(Top)** β -D-Glucose **1** and complementary receptor framework **2**. Polar and hydrophobic moieties are shown in red and blue, respectively. X can be varied to control solubility. Versions of **2** are described in (19–21). **(Bottom)** Disaccharide receptor **3**, reported herein, and cellobiose **4**, an intended substrate. The roof and floor of **3** are provided by *meta*-terphenyl units (blue). There are five isophthalamide pillars, two at either end (red) and one located centrally (magenta). The water-solubilizing tricarboxylate units are shown in green. The molecule has two planes of symmetry, one lying parallel to and between the terphenyls, and the other passing through the central (magenta) isophthalamide.

Fig. 2. Evidence for complex formation between receptor **3** and cellobiose **4**. **(A)** Partial ^1H NMR spectra from the addition of **4** to **3** in D_2O . The signals shown are due to receptor aromatic protons. The concentration of **3** = 0.5 mM. **(B)** ICD caused by the addition of **4** (0 to 7 mM) to **3** (0.25 mM). λ , wavelength. **(C)** Increase in fluorescence output caused by the addition of **4** (0 to 9 mM) to **3** (0.01 mM). CPS, counts per second. **(D)** Analysis of data from (C) by nonlinear least-squares curve fitting, assuming 1:1 binding stoichiometry. $K_a = 560 \text{ M}^{-1}$, limiting $\Delta\text{CPS} = 320$ CPS. Observed and calculated points are almost coincident.

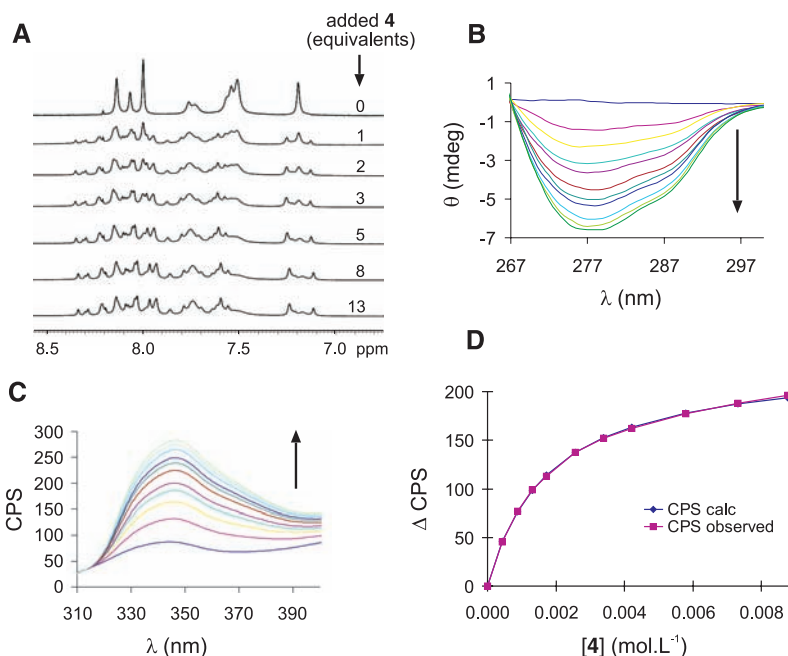


Table 1. Binding constants of carbohydrates to **3** in aqueous solution, as measured by ^1H NMR, ICD, and fluorescence titrations. Aqueous solution is defined as D_2O for the NMR measurements and H_2O for CD and fluorescence. $T = 298\text{ K}$, except where indicated. ND indicates not done. For structural formulas of **5** to **16**, see Fig. 4.

Carbohydrate	K_a (M^{-1})		
	^1H NMR	ICD	Fluorescence
D-Cellobiose (4 , $1\beta\text{-OH}:1\alpha\text{-OH} = 3:2$)	$600^*\S$	580	560
Methyl $\beta\text{-D}$ -cellobioside (5)	‡	910	850
D-Xylobiose (6)	‡	250	270
D- N,N' -diacetylchitobiose (7)	120^*	ND	120
D-Lactose (8)	‡	11	14
D-Mannobiose (9)	‡	13	9
D-Maltose (10)	‡	15	11
D-Gentiobiose (11)	ND	12	5
D-Trehalose (12)			ND
D-Sucrose (13)	ND		
D-Glucose (14)	$11^\dagger\S$	12	
D-Ribose (15)	ND		
D- N -acetylglucosamine (16)	24^\dagger	ND	19

*Slow exchange on the NMR time scale. †Fast exchange on the NMR time scale. ‡Intermediate exchange (leading to broad peaks and preventing the determination of K_a). § $T = 278\text{ K}$. ||No change in spectrum upon addition of carbohydrate.

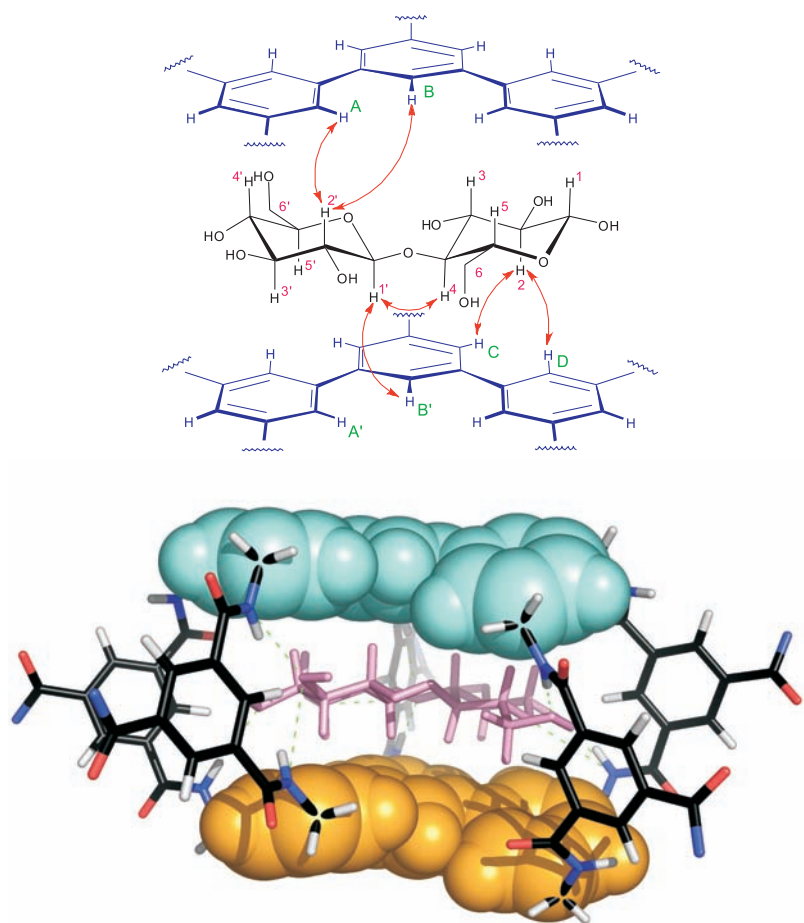


Fig. 3. (Top) NOESY contacts observed for the complex between β -cellobiose and receptor **3**. (Bottom) A computational model of the complex, consistent with the NOE data. Water-solubilizing side chains are omitted for clarity. The cellobiose is colored pink, and the terphenyl units are shown in space-filling mode. Polar interactions are represented as dotted lines. Black, carbon; red, oxygen; blue, nitrogen; and white, hydrogen.

rotating-frame nuclear Overhauser effect spectroscopy (ROESY) shows chemical-exchange cross peaks linking bound and unbound cellobiose chemical shifts, so that the shifts for the bound carbohydrate could be determined (figs. S7 to S9). Cellobiose in solution consists of a 2:3 mixture of α and β anomers (**4a** and **4b**), with the C1–OH group in the axial and equatorial orientations, respectively. For **4b**, a full set of cross peaks was observed, and a complete assignment was therefore possible (table S1). All the carbohydrate protons moved upfield upon binding, by amounts between 0.5 and 2.1 parts per million. Such changes are consistent with the expected structure, in which the disaccharide is sandwiched between the aromatic surfaces.

Results from nuclear Overhauser effect spectroscopy (NOESY) further support this mode of binding. A strong cross peak between the cellobiose 1' and 4 protons established that the glycosidic linkage was in the syn conformation (32), giving the required flat profile (Fig. 3). Intermolecular cross peaks were observed between aromatic receptor signals and all carbohydrate chemical shifts (fig. S10). The involvement of protons from both faces of the disaccharide provides clear proof of encapsulation. The aromatic region of the spectrum was too crowded for a comprehensive analysis but a few contacts could be identified unambiguously (Fig. 3). Strong NOE signals of similar intensities were observed between H2' and two protons in the crescent of the terphenyl (A and B in Fig. 3). A similar pair of contacts were detected between H2 and two exterior terphenyl protons (C and D in Fig. 3). A further strong NOE was found between H3' and the terphenyl HA', and a weaker signal was observed between H1' and HB'. The 2'–A/B contacts were used as constraints for molecular modeling, in which a Monte Carlo molecular mechanics search was performed with both distances held at 2.5 Å, and then the resulting conformations were remimized with no constraints (27, 28). The baseline structure is shown in Fig. 3. It retains the 2'–A/B contacts (2.63 and 2.87 Å) while independently predicting the 2–C/D contacts (2.58 and 2.78 Å), the 3'–A' proximity (3.04 Å), and the longer 1'–B' distance (3.44 Å). The structure features 8 intermolecular hydrogen bonds and ~ 10 CH– π interactions and seems a persuasive model for the complex. The chiral guest imparts a twist to the host, consistent with the observed ICD.

The NMR spectra were also examined for evidence of binding to **4a**. Again, the ROESY spectra showed cross peaks between bound and unbound carbohydrate, allowing for the assignment of most disaccharide protons (table S2). However, NOESY spectra suggest that the binding was weaker. If so, the affinity for **4b** must be greater than the measured value of $\sim 600\text{ M}^{-1}$, considering that this figure is an average for the two anomers.

To assess its selectivity, receptor **3** was tested against 10 disaccharides and 3 monosaccharides

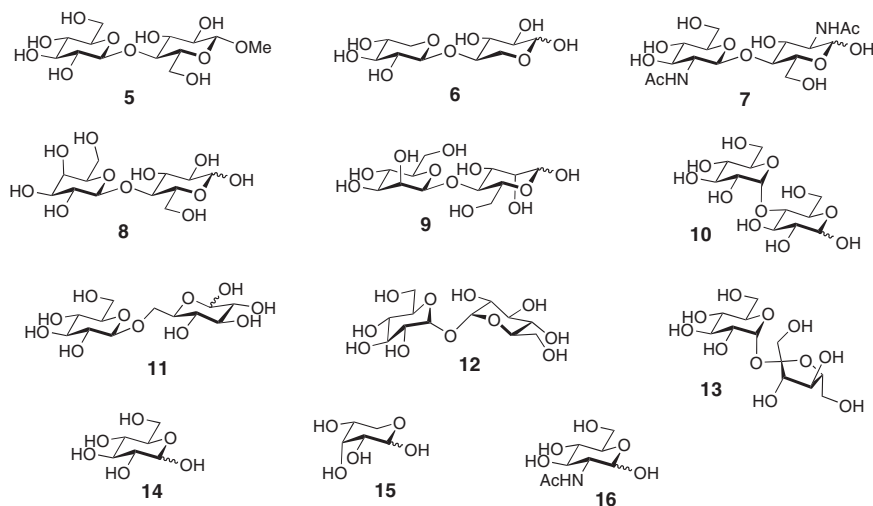


Fig. 4. Carbohydrate substrates used with receptor **3** (in addition to cellobiose **4**). For binding results, see Table 1. Me, methyl; Ac, acetyl.

(Fig. 4 and Table 1) (29). At least two techniques were applied in each case (33). Agreement between the methods was generally good. Methyl β -D-cellobioside **5** might be seen as a model for **4** and was bound with $K_a \sim 900 \text{ M}^{-1}$. Two closely related all-equatorial disaccharides, xylobiose **6** and N,N' -diacetylchitobiose **7**, were complexed somewhat less strongly ($K_a = 260$ and 120 M^{-1} , respectively). Of the remaining substrates, the highest value was $\sim 20 \text{ M}^{-1}$ (for N -acetylglucosamine **16**). Most remarkable were the results for lactose **8** and gentiobiose **11**. The former possesses just one axial OH group, the latter an all-equatorial structure that is slightly longer than **4**. In both cases, the change from **4** was enough to reduce the binding constant to $\sim 12 \text{ M}^{-1}$. Indeed, the selectivity for **4** versus nontargeted disaccharides was generally $\sim 50:1$ or better.

The ^1H NMR measurements also provided information about binding kinetics. Whereas binding to **4** and **7** was slow on the NMR time scale, exchange of the other substrates was intermediate or fast (Table 1). This behavior lies within the range for lectins, which can show fast or slow exchange by NMR (34, 35). The differing exchange rates were exploited in a competition experiment that confirmed the receptor's selectivity for cellobiose **4**. The addition of eight nontarget substrates (**8** and **10** to **16**; 20 mM each) to **3** caused broadening and shifting of the receptor ^1H NMR signals, as is expected for intermediate or fast exchange (fig. S52). However, upon further addition of only 9 mM **4**, these signals were replaced almost quantitatively by the spectrum of complex **3-4**. The cellobiose complex was thus formed nearly exclusively in the presence of an 18-fold excess of nontarget carbohydrate. The experiment shows that, like a natural lectin, receptor **3** can bind its target from a complex mixture of potential substrates.

In terms of affinity, receptor **3** cannot match the highest values found in nature (36). How-

ever, the K_a value for β -cellobiosyl (approaching 10^3 M^{-1}) is comparable to that for many carbohydrate/protein interactions (9). Moreover, the specificity of **3** for a narrow class of substrates is high, even by biological standards. This performance is achieved with a system that is far smaller than a typical lectin. The sense of selectivity accords with the design, which was specifically aimed at all-equatorial disaccharides. The targets **4**, **6**, and **7** relate to important biopolymers. Cellobiose **4** is the repeat unit of cellulose, the most abundant organic material on earth and a major renewable resource. Xylobiose **6** and N,N' -diacetylchitobiose **7** are representative of xylan and chitin, the most abundant polysaccharides after cellulose. Both are important resources, and chitin is a potential target for insecticides and antifungal agents (37). Further work may lead to molecules that can bind the polymers themselves, with potential for applications in processing (e.g., solubilization) and biomedical research.

Synthetic lectins could also be immobilized and used to separate carbohydrates or glycoconjugates, or they could be fitted with transducing elements (such as fluorophores) to give specific saccharide sensors. In the shorter term, receptor **3** provides a realistic model for carbohydrate-binding proteins. Affinities, selectivities, thermodynamic parameters, and kinetic properties all lie within the spread of values observed for lectins. At the same time, the receptor possesses a robust, covalently enforced binding cavity. This should allow studies under conditions that would denature proteins, adding an important tool for exploring the principles underlying biological carbohydrate recognition.

References and Notes

- A. P. Davis, T. D. James, in *Functional Synthetic Receptors*, T. Schrader, A. D. Hamilton, Eds. (Wiley-VCH, Weinheim, Germany, 2005), pp. 45–109.
- A. Lutzen, in *Highlights in Bioorganic Chemistry: Methods and Applications*, C. Schmuck, H. Wennemers, Eds. (Wiley-VCH, Weinheim, Germany, 2004), pp. 109–119.

- A. P. Davis, R. S. Wareham, *Angew. Chem. Int. Ed.* **38**, 2978 (1999).
- S. Striegler, *Curr. Org. Chem.* **7**, 81 (2003).
- H. J. Gabius, H. C. Siebert, S. Andre, J. Jimenez-Barbero, H. Rudiger, *ChemBioChem* **5**, 740 (2004).
- R. A. Dwek, T. D. Butters, *Chem. Rev.* **102**, 283 (2002).
- C. R. Bertozzi, L. L. Kiessling, *Science* **291**, 2357 (2001).
- J. J. Lundquist, E. J. Toone, *Chem. Rev.* **102**, 555 (2002).
- E. J. Toone, *Curr. Opin. Struct. Biol.* **4**, 719 (1994).
- We use the term "biomimetic" for recognition employing noncovalent interactions. An alternative, "nonbiomimetic" approach to carbohydrate binding involves the reversible formation of boronate esters (1, 11).
- T. D. James, M. D. Phillips, S. Shinkai, *Boronic Acids in Saccharide Recognition* (Royal Society of Chemistry, Cambridge, 2006).
- O. Francesconi, A. Ienco, G. Moneti, C. Nativi, S. Roelens, *Angew. Chem. Int. Ed.* **45**, 6693 (2006).
- M. Waki, H. Abe, M. Inouye, *Chem. Eur. J.* **12**, 7839 (2006).
- M. Mazik, A. König, *J. Org. Chem.* **71**, 7854 (2006).
- C. Nativi *et al.*, *J. Am. Chem. Soc.* **129**, 4377 (2007).
- M. Mazik, H. Cavga, *J. Org. Chem.* **71**, 2957 (2006).
- C. Schmuck, M. Schwegmann, *Org. Lett.* **7**, 3517 (2005).
- For earlier, organic-soluble versions, see (19, 20).
- A. P. Davis, R. S. Wareham, *Angew. Chem. Int. Ed.* **37**, 2270 (1998).
- T. J. Ryan, G. Lecollinet, T. Velasco, A. P. Davis, *Proc. Natl. Acad. Sci. U.S.A.* **99**, 4863 (2002).
- E. Klein, M. P. Crump, A. P. Davis, *Angew. Chem. Int. Ed.* **44**, 298 (2005).
- Although monosaccharides have attracted more attention, a few synthetic receptors have been aimed at oligosaccharides (1–3, 11, 14, 15, 23–26).
- U. Neidlein, F. Diederich, *Chem. Commun.* **1996**, 1493 (1996).
- R. D. Hubbard, S. R. Horner, B. L. Miller, *J. Am. Chem. Soc.* **123**, 5810 (2001).
- G. Lecollinet, A. P. Dominey, T. Velasco, A. P. Davis, *Angew. Chem. Int. Ed.* **41**, 4093 (2002).
- O. Alpturk *et al.*, *Proc. Natl. Acad. Sci. U.S.A.* **103**, 9756 (2006).
- Monte Carlo molecular mechanics calculations were performed using MacroModel 9.0 (Maestro 7.0 interface) with the Merck Molecular Force Field (static) and Generalized Born/Surface Area (water) continuum solvation.
- MacroModel 9.0 (Maestro 7.0 interface), supplied by Schrödinger, Portland, OR; www.schrodinger.com.
- For further details, see the Supporting Online Material.
- W. Blokzijl, J. B. F. N. Engberts, *Angew. Chem. Int. Ed. Engl.* **32**, 1545 (1993).
- H. Lis, N. Sharon, *Chem. Rev.* **98**, 637 (1998).
- E. A. Larsson, M. Staaf, P. Soderman, C. Hoog, G. Widmalm, *J. Phys. Chem. A* **108**, 3932 (2004).
- In some cases, experimental problems precluded the use of a technique. For example, some substrates gave broad NMR spectra because of intermediate exchange rates, whereas others possessed sufficient CD activity to interfere with ICD measurements.
- N. Aboitiz *et al.*, *ChemBioChem* **5**, 1245 (2004).
- K. J. Neurohr, N. M. Young, I. C. P. Smith, H. H. Mantsch, *Biochemistry* **20**, 3499 (1981).
- S. M. Koning, M. G. L. Elferink, W. N. Konings, A. J. M. Driessen, *J. Bacteriol.* **183**, 4979 (2001).
- T. Theis, U. Stahl, *Cell. Mol. Life Sci.* **61**, 437 (2004).
- This work was supported by European Commission Research Training Network contract HPRN-CT-2002-00190 and Engineering and Physical Sciences Research Council grant EP/D060192/1. A.P.D. dedicates this paper to the memory of Peter Davis.

Supporting Online Material

www.sciencemag.org/cgi/content/full/318/5850/619/DC1
Materials and Methods
SOM Text
Figs. S1 to S52
Tables S1 and S2
References

2 August 2007; accepted 17 September 2007
10.1126/science.1148735